EMPIRICAL FORMULAS FOR LOCATING SHOCK WAVES IN A JET IMPINGING ON A BARRIER AT RIGHT ANGLES

B. G. Semiletenko and V. N. Uskov

UDC 532.525.2:533.6.011.72

Empirical relations are derived for determining the ranges of stable and unstable interaction between a jet and a barrier and for determining the displacement of the central compression shock and of the triple point from the barrier.

The authors generalize here the results of experimental studies concerning the wave structure in a jet impinging on an infinitely large flat barrier located within the initial jet region perpendicularly to the jet axis. The tests were performed with air jets discharging from conical nozzles (diameter of the exit section d_e = 12, 20 mm and semivertex angles ϑ_v = 5, 17°). The Mach number at the exit section of the nozzles was Ma = 1-3, the inefficiency ratio $n = p_e/p_a$ varied from 1.2 to 36. Photographs of the wave structure before the barrier were taken with the aid of a model IAB-451 optical device (Tepler instrument). The static and the stagnation pressures at the barrier were measured with model DD-10 inductive probes of the model ID-2I instrument set. The probe readings were recorded on a model N-115 loop oscillograph. A detailed description of the test stand, the instrumentation, the test procedure, and the data processing was given in [1]. The results were compared with certain test data on the interaction between high-temperature jets.

The interaction between a supersonic jet with a barrier is characterized by the occurrence of a central compression shock 4 in the jet before the barrier (Fig. 1). An intersection between the central shock 4 and a dropping shock 5 results in a reflected shock 6 and the formation of a tangential discontinuity surface 7 (i.e., the formation of a triple node at point T). The tangential discontinuity surface separates the subsonic flow behind the central compression shock from the ordinary supersonic flow behind the reflected shock. The structure of shock waves in the jet varies with the distance h as follows:

1) The compression shock curves toward the nozzle, at distances h approximately equal to the distance from the nozzle throat to the point where the first characteristic originating at the nozzle edge intersects the nozzle axis.

2) With increasing distances h, the central compression shock may pass through inflections and then curves toward the barrier.

3) With still larger distances h, the flow becomes unstable ($h = h_{ii}$) [1, 2]. The wave structure in the jet before the barrier fluctuates at a high frequency and appears very smudgy on the photographs. The unstable mode of interaction between jet and barrier is accompanied by a generation of strong acoustic waves in the surrounding space. Pressure measurements [1, 2] have shown that the occurrence of a strong instability is related to the appearance of a peripheral pressure peak at the barrier. No breakdown of the wave structure was noted at high values of the inefficiency ratio n, although the static pressure peaked out at the barrier.

4) As the distance h between barrier and nozzle increases further, the instability of the wave structure abates, until at some distance the compression shocks become stable. According to Fig. 2, where I represents the zone of strong instability, the range of distances h at which strong instabilities occur narrows down with increasing inefficiency ratio.

Institute of Mechanics, Leningrad. Translated from Inzhenerno-Fizicheskii Zhurnal, Vol. 23, No. 3, pp. 453-458, September, 1972. Original article submitted April 7, 1971.

© 1974 Consultants Bureau, a division of Plenum Publishing Corporation, 227 West 17th Street, New York, N. Y. 10011. No part of this publication may be reproduced, stored in a retrieval system, or transmitted, in any form or by any means, electronic, mechanical, photocopying, microfilming, recording or otherwise, without written permission of the publisher. A copy of this article is available from the publisher for $15.00.

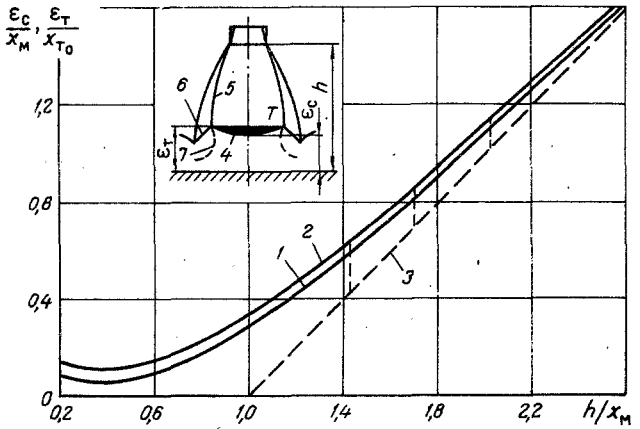

Fig. 1. Displacement of compression shock ε_c and of triple point ε_T from the barrier: ε_c (1), ε_T (2), $\varepsilon/x_M = h/x_M - 1$ (3), central compression shock (4), dropping compression shock (5), reflected compression shock (6), tangential discontinuity (7).

5) During certain modes of jet discharge there is an interval of second instability ($h = h_{2i}$) (Fig. 2, zone II). The acoustic field and the fluctuations of the wave structure are much weaker here than during the first instability mode.

6) The weak instability is followed by a stepwise transition to stable interaction between jet and barrier ($h = h_*$). Here the structure of shock waves corresponds to the position of shock waves in the first "roll" in an immersed jet, and before the barrier there appears a second central compression shock. A peripheral pressure peak at the barrier occurs within the entire interval of distances $h_{1i} \leq h \leq h_*$. At high inefficiency ratios such a peak will occur also when $h \geq h_*$.

The general features of this trend in the variation of the wave structure were observed throughout the entire range of parameter values during jet discharge from the nozzles. Depending on Ma and n, however, each of the h intervals had its peculiar characteristics. These have been analyzed thoroughly in [1, 2].

Pressure measurements at the barrier and processing of over 250 Tepler photographs have yielded certain empirical formulas for finding the location of shock waves in a jet before a barrier, as a function of the jet discharge parameters (Ma, d_e, k, n) and the distance h from the nozzle throat section to the barrier. The maximum relative error in measuring the linear dimensions on the photographs did not exceed 2%.

The graph in Fig. 3 represents the relation between the barrier position at the start of the first (strong) flow instability and the jet discharge parameters. The values of h_{1i} were determined from Tepler

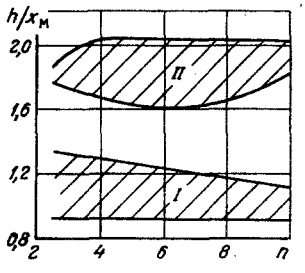

Fig. 2

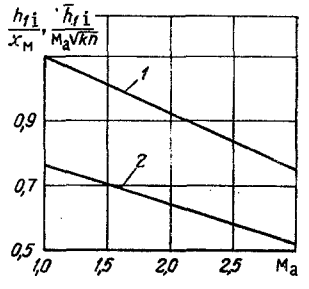

Fig. 3

Fig. 2. Boundaries of unstable interaction between jet and barrier, at Ma = 2, k = 1.4, $\vartheta_V = 5°$: zone of strong instability (I), zone of weak instability (II).

Fig. 3. Start of a strong instability (appearance of a peripheral pressure peak): according to Eq. (1) (1), according to Eq. (1') (2).

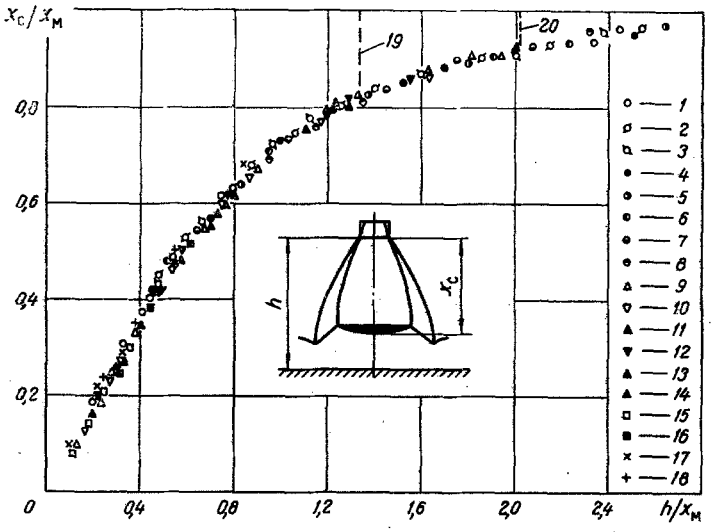

Fig. 4. Some test values for the distance from the nozzle exit section to the central compression shock (x_c): Ma = 1.0 and n = 36.0 (1), 31.4 (2), 26.2 (3), 15.9 (4), 7.55 (5), Ma = 1.5 and n = 20.8 (6), 15.9 (7), 5.1 (8), Ma = 2.0 and n = 9.8 (9), 7.55 (10), 5.1 (11), Ma = 2.5 and n = 5.1 (12), 2.45 (13), Ma = 3.0 and n = 2.45, k = 1.25, $\vartheta_v = 17°$ (14), Ma = 2.0 and n = 25 (15), 15 (16), Ma = 3.0 and n = 4 (17), 2.5 (18), transition to $x_c/x_M = 1$ at Ma = 3.0 and n = 2.45 (19), at Ma = 2.0 and n = 9.8 (20).

photographs (h_{1i} representing the distance at which the wave structure in the jet before the barrier began to break down) as well as from the distribution of static pressure at the barrier (based on the appearance of a peripheral pressure peak). The values of h_{1i} have been referred here to the corresponding distance x_M from the nozzle to the Mach circle in an immersed jet (line 1) (the values of x_M were measured on Tepler photographs of immersed jets) or to the quantity $d_e Ma\sqrt{kn}$ (line 2). The test values of h_{1i} were obtained at Ma = 1.0, 1.5, 2.0, 2.5, and 3.0 over a wide range of n. For each value of Ma we obtained at least 10 values of h_{1i}/x_M from which then the mean value h_{1i}/x_M was found by averaging. The standard deviation of points from this mean value did not exceed 0.02 for all Mach number values. The following lines were fitted through the test points (Fig. 3):

$$\frac{h_{1i}}{x_M} = 1.26 - 0.17 Ma, \tag{1}$$

$$\frac{h_{1i}}{d_e Ma\sqrt{kn}} = 0.88 - 0.12 Ma. \tag{1'}$$

The standard deviation of points was $\sigma' = 0.028$ from line 1 and $\sigma'' = 0.020$ from line 2.

Displacements of the central compression shock ε_c and of the triple point ε_T from the barrier surface are shown in Fig. 1. The magnitudes of these displacements have been referred to the distance from the Mach circle x_M as well as to the abscissa of the triple point (x_{T_0}) in an immersed jet. The distance to the barrier has been referred to x_M. In order to plot this curve from Tepler photographs, we measured the distances from the nozzle to the central compression shock x_c and to the triple point x_T. The relation $x_c/x_M = f(h/x_M)$ is shown in Fig. 4. The compression shock during unstable modes of jet and barrier interaction appeared smudgy on the photographs and, for this reason, its location within these ranges of h have not been plotted on the curve. Since the instability modes occur at different values of h/x_M, depending on Ma and n, and those for large values of n have not been recorded, hence the test points fit on the curve here smoothly. The curve of x_c/x_M as a function of h/x_M approaches unity smoothly, but at the distance h_* there occurs for each discharge mode (i.e., for each value of Ma and n) a jumpwise transition from the curve to the straight line $x_c/x_M = 1$. As an example, such transitions are shown in Fig. 4 by dashed lines for Ma = 3.0, 2.0 and n = 2.45, 9.8 respectively. A similar graph had been plotted in [3], but there the h values were referred to h_*. However, the curve obtained by the authors of [3] has, in our opinion, several shortcomings:

1. Since it is rather difficult to determine the value of h_* from the jet discharge parameters, hence that graph cannot be used for calculating the shock displacement.

2. Our results indicate that $x_c/x_M = f(h/x_M)$ cannot approach the $x_c/x_M = 1$ line continuously.

3. An evaluation of our data in coordinates proposed by the authors of [3] has resulted in a scatter of test points with respect to Mach number values.

The displacement of the central compression shock in hot jets ($T_0 = 2800°K$, $k = 1.25$) is determined from pressure readings at the center of the barrier. The pressure at the center of the barrier was assumed here equal to the total pressure behind the central compression shock — an assumption which had been verified experimentally. Knowing the total pressure before and behind the central compression shock, and knowing the Mach number distribution along the jet axis [4], one can locate the shock in the jet before the barrier. The values thus obtained are shown in Fig. 4. The $x_c/x_M = f(h/x_M)$ curve was calculated on a "Promin'" computer by the method of least squares. The relation $\varepsilon_c = h - x_c$ has yielded an empirical equation for the shock displacement ε_c from the barrier surface:

$$\frac{\varepsilon_c}{x_M} = \frac{h}{x_M} - 1 + 1.13 \exp\left(-1.36 \frac{h}{x_M}\right). \tag{2}$$

By the same procedure we derived the more convenient formula

$$\frac{\varepsilon_c}{d_e M_a \sqrt{kn}} = \frac{h}{d_e M_a \sqrt{kn}} - 0.745 + 0.83 \exp\left(-1.73 \frac{h}{d_e M_a \sqrt{kn}}\right). \tag{2'}$$

The mean-squared errors of formulas (2) and (2') are $\sigma = 0.015$ and 0.024 respectively, i.e., with a 95% probability level the confidence intervals are 0.03 and 0.048 respectively.

Analogous equations have been derived for the displacement of the triple point from a barrier:

$$\frac{\varepsilon_T}{x_{T_0}} = \frac{h}{x_M} - 1 + 1.18 \exp\left(-1.28 \frac{h}{x_M}\right), \quad \sigma = 0.020 \tag{3}$$

and

$$\frac{\varepsilon_T}{d_e M_a \sqrt{kn}} = \frac{h}{d_e M_a \sqrt{kn}} - 0.72 + 0.88 \exp\left(-1.75 \frac{h}{d_e M_a \sqrt{kn}}\right), \tag{3'}$$

$$\sigma = 0.020.$$

At distances $h > h_*$ the wave structure of the first "roll" is unperturbed, i.e., $x_c = x_M$ and the straight line in Fig. 1 is described by the equation $\varepsilon_c/x_M = h/x_M - 1$. The transition to an unperturbed first "roll" occurs jumpwise and, therefore, according to Fig. 1, at distances $h = h_*$ such are the transitions from curves 1 and 2 to the straight line 3.

The distances h_* were determined not only from Tepler photographs of a jet impinging on a barrier but also more precisely from pressure measurements at the center point of the barrier [1]. Under the same gasodynamic conditions at the nozzle exit section, at increasing distances h the pressure at the center point decreases until $h = h_*$. When $h = h_*$, there appears before the barrier a second central compression shock and at the center point of the barrier one notes a pressure spike. For this reason, the distance h_* is more conveniently determined from pressure spikes on the oscillogram rather than from photographs. An analysis of the results has shown that at $n \geq 4$ the distance h_* can be calculated by the formula

$$\frac{h_*}{d_e \sqrt{kn}\, M_a} = 2.05 - 0.003. \tag{4}$$

with a mean-squared error 0.034.

For $n < 4$ the test points do not fit on a single straight line but they scatter, instead, with respect to the Mach number values. The curves which correspond to the lower values of the Mach number have a larger positive slope.

The empirical equations derived here render an approximate description of the wave structure in a jet before a barrier, if the jet parameters at the nozzle exit section (Ma, d_e, n, k) are known.

NOTATION

Ma is the Mach number;

d_c is the diameter of nozzle exit section;
ϑ_v is the nozzle semivertex angle;
n is the inefficiency ratio;
p_c is the static pressure at the nozzle exit section;
p_a is the ambient static pressure;
h is the distance from nozzle throat to barrier;
h_{1i} is the start of the first (strong) instability;
h_{2i} is the start of the second (weak) instability;
h_* is the transition to a flow with an unperturbed first "roll" in the jet;
x_M, x_{T_0}, x_c, x_T are the distance from the nozzle throat to the Mach circle, to the triple point in a free jet, to the central compression shock, and to the triple point respectively;
ε_c, ε_T are the displacement of the compression shock and of the triple point from a barrier.

LITERATURE CITED

1. I. P. Ginzburg, B. G. Semiletenko, and V. N. Uskov, Scientific Notes of the Leningrad State University, in: Gasodynamics and Heat Transfer [in Russian] (1972), No. 3.
2. I. P. Ginzburg, B. G. Semiletenko, V. S. Terpigor'ev, and V. N. Uskov, Inzh. Fiz. Zh., 19, No. 3 (1970).
3. A. K. Poluboyarinov and N. I. Spirin, Inzh. Fiz. Zh., 18, No. 2 (1970).
4. V. A. Zhokhov and A. A. Khomutskii, Trudy TsAGI, No. 1224 (1970).